TOPICS IN LANDING GEAR DYNAMICS RESEARCH AT NASA LANGLEY

ICAS-86-5.9.4

Harvey G. McComb, Jr. and John A. Tanner
NASA Langley Research Center
Hampton, Virginia 23665-5225

Abstract

Four topics in landing gear dynamics are discussed. Three of these topics are subjects of recent research: tilt steering phenomenon, water spray ingestion on flooded runways, and actively controlled landing gear. The fourth topic is a description of a major facility recently enhanced in capability.

I. Introduction

Research on aircraft landing gear dynamics has been performed at Langley Research Center for over 30 years. Topics addressed during this period include tire mechanics, tire friction and cornering forces, tire wear, hydroplaning, runway and highway grooving, brake dynamics, antiskid system performance, and air cushion landing gear. The purpose of this paper, however, is not to review all these activities; rather four topics have been selected for discussion because of timeliness and perceived general interest. Three of these topics are subjects of recent research. The fourth deals with a major facility recently enhanced in capability.

First, the tilt steering phenomenon is addressed, in which significant side forces can be generated by free-swiveling nose wheels if the landing gear strut is tilted from the vertical because of cross-winds or runway crown. This phenomenon is important when differential braking of main landing gear is used to steer an aircraft, a situation common to fighter aircraft, for example.

Second, research on water spray generated by a nose wheel when operating on a flooded runway is discussed. Careful experimentation has revealed these spray patterns for general aviation type aircraft. This work is important in understanding spray ingestion by turbine engines particularly if the engines are located on the rear of the fuselage.

Third, status of research on actively controlled landing gear is discussed. Experimental and analytical research has determined that installation of an active element in a landing gear strut can reduce fatigue damage and improve ride quality in ground operations. Research in this area has reached the stage where a flight test is planned to validate the technology.

Finally, the Aircraft Landing Dynamics Facility (ALDF) is discussed. The ALDF consists of a 0.8 km (0.5 mile) long track with a carriage propelled by an external water jet. Test articles are mounted on the carriage. The facility was recently enhanced to double the maximum speed capability and increase the size of test article which can be handled. The paper closes with a brief description of the facility and planned research.

II. Tilt Steering Phenomenon

Mechanical properties of tires sometimes lead to forces not normally anticipated. When a tire rotates in a tilted or cambered condition and is free to swivel about the steering axis, a side force or cornering force is produced. This phenomenon was clearly observed during landing gear tests in 1966 on a model of an HL-10 manned lifting entry vehicle[1]. It has also been addressed in recent research [2,3]. The phenomenon is associated with the way local friction forces in the tire footprint combine to form resultant forces at the tire-runway interface[2]. The effect is related to the fact that, when the landing gear is tilted, the rotation radius at one edge of the tire footprint (R_{inner}) is less than the radius at the other edge of the footprint (R_{outer}) as indicated in Figure 1. As the wheel and tire rotate about the axle, the tendency is to behave like a cone rather than like a cylinder. This turning tendency causes a cornering or side force to be developed.

Tests were conducted at Langley to study the tilt steering phenomenon. Effects of various parameters on the magnitude of cornering forces were measured. These parameters included tilt angle, trail, tire inflation pressure, rake angle, vertical load, and, in the case of a twin-tire arrangement, whether the wheels are locked together (corotating) or rotate independently. Two test vehicles were used--a modified airboat shown in Figure 2 which is a versatile test frame for landing gear research[2], and an F-106 fighter aircraft[3]. Tests were subsequently conducted on a Space Shuttle Orbiter[3].

To measure side or cornering forces the test vehicles were not operated under their own power, but rather were towed in an arrangement shown in Figure 3. The tow tug and instrumentation tug are simply small service vehicles used to tow aircraft around the hangar area for servicing. The force transducer is a strain-gage-type load cell which measures the load in the cable between the test vehicle nose gear and the instrumentation tug. The tugs are driven in a straight line--the technique of following expansion joints in the hangar apron pavement was effective. The tests were conducted at low speeds, and further research is required to determine effects of ground speed. Selected results from the airboat tests are shown in Figure 4. These results are for twin-wheel nose gear with two values of trail indicated on Figure 4 and either independent rotating wheels or corotating wheels. Cornering force coefficient is simply the cornering force measured at the nose gear divided by the vertical load on the nose gear. In Figure 4 the cornering force coefficient is plotted as a function of tilt angle. These results show that the corotating twin-wheel nose gear can exhibit substantially larger cornering force coefficients than the independently rotating twin-wheel wheel nose gear.

Tests on the F-106 aircraft are pictured in Figure 5. The tug in the distance in Figure 5 is

the tow tug, the one on the right is the instrumentation tug, and the tug on the left is a braking tug used to prevent the test aircraft from overrunning the tow tug. Results are presented in the next paragraph in conjunction with Shuttle Orbiter results.

For most Space Shuttle missions the nose landing gear has operated in a free castering mode during Orbiter landing runout--steering on the ground has been accomplished by differential braking on the main landing gear. The towing arrangement shown in Figure 3 was applied to the Space Shuttle Orbiter to measure the cornering force on the nose gear of that vehicle. The test setup for the Orbiter is shown in Figure 6. Comparison between the F-106 fighter results and the shuttle Orbiter results are shown in Figure 7. The Orbiter has corotating nose wheels whereas the F-106 has independently rotating nose wheels. Again, the disparity between these nose wheel rotation conditions is evident in Figure 7. Nose gear steering is now operational on all Orbiters, and it is expected to be used on all future flights.

III. Spray Ingestion

Some aircraft experience engine problems or flameouts due to water spray or slush from nose wheels being ingested when operating on flooded runways. The problem is more likely to occur on aircraft with rear mounted engines (see Fig. 8). The objective of this research was to define the trajectory and measure the flow rate of spray from an aircraft nose wheel for the variable parameters of speed, tire deflection, water depth, and with the presence of fuselage aerodynamics.

The tests were conducted in a towing tank 878 m (2,880 ft) long, 7.3 m (24 ft) wide, and 3.7 m (12 ft) deep. The test article is mounted on a 16,330 kg (36,000 lbm) carriage capable of speeds up to 24 m/s (80 ft/s). The test article was a Navajo aircraft wing, fuselage, and nose wheel. A test runway 15 m (50 ft) long and 0.9 m (3 ft) wide with small flanges along the edges to control water depth up to 1.6 cm (5/8 in.) was constructed in the tank.

A photograph of a typical run in the tank is shown in Figure 9. Two data gathering systems were used in the test program. Motion picture cameras were used to define spray trajectory, and an array of water collection tubes was used to catch the water for flow rate measurements (see Fig. 10). The water leaves the tire in the form of a solid sheet, but as time progresses the sheet breaks up into droplets which continue to rise as they lose speed and finally enter the collector or fall to the ground. As the tire passes through a flooded runway, a wake is set up much the same as from a speeding boat on a lake. This wake, like the tire, has enough energy to throw water into the air, so that a much larger volume of water, perhaps as much as 5-10 times greater than that displaced by the tire alone, is displaced and may eventually find its way into the engine.

Water spray coming from a tire appears to move aft as the tire moves through the puddle. This perception is an illusion created by the motion of the vehicle and the fact that the spray frequently is viewed from the moving vehicle itself. A study of the movie film from stationary cameras indicates that water particles coming from a tire move upward approximately 45 degrees and forward approximately 10 degrees as shown in Figure 11. Trajectory angles of water particles were found to be relatively constant for the speed range and water depth studied. It was also found that the speed of water particles leaving the tire was higher than the speed of the tire itself. For the run shown in Figure 11, for example, the test tire speed was 12 m/s (40 ft/s) but the speed of the water leaving the tire was approximately 20 m/s (65 ft/s).

A contour map typical of flow rate measurements made in this research is shown in Figure 12. These particular results were from a test of wheel and tire alone (i.e. no wing and fuselage present). The view is a rear view (looking forward), and the test tire was located off the lower left hand corner of the map (see dashed sketch in Figure 12). The map represents a square plane 1.6 m (63 in.) on edge located 5.05 m (16.6 ft) aft of the test wheel axle and oriented normal to the longitudinal axis of the aircraft. The left edge of the map is approximately on the center-line of the test tire, and the bottom edge is 0.41 m (16 in.) above the ground. The spray pattern moves diagonally from lower left to upper right corner of the map. The contour lines represent flow rate increments of 10 ml/s. Engine performance can be affected by the flow rates of water ingested, and these data provide a way of estimating such flow rates.

IV. Actively Controlled Landing Gear

Aircraft dynamic loads and vibrations resulting from landing impact and from runway and taxiway unevenness are recognized as significant factors in causing fatigue damage and dynamic stress on airframe and crew and passenger discomfort. In addition, in large flexible aircraft the ability of the pilot to control the aircraft during ground operations may be affected. A potential method to reduce these loads is application of active control technology to landing gear design.

A mathematical model of an active landing gear was developed and programmed for digital computer operation[4]. The model contains an electronic controller which positions a quick-reacting fluid-controlling servo-valve to limit airplane mass-center force to a minimum compatible with the available shock-strut stroke and the airplane kinetic energy. This minimum mass-center force is called the limit force. As long as the mass-center force is greater than the limit force, the control system removes fluid from the strut at a rate which varies with the magnitude of the force difference. As the mass-center force decreases toward the limit force, the control system reduces the rate at which fluid is removed and when the mass-center force becomes less than the limit force, fluid is added to the strut. This process is continued until a static value of shock strut extension and hydraulic pressure is reached at equilibrium. Detailed analytical and computer modeling studies, using the developed control laws, showed that the active gear reduces forces transmitted to the airframe during landing impact, and during subsequent roll-out and taxi operations over rough runways.

To assess the feasibility and potential of the actively controlled gear concept, an experimental study was performed[5]. A main landing gear strut from a general aviation light-twin

aircraft was modified for use in an active-control mode. A schematic of the modified strut system is in Figure 13. To provide the necessary conduit for hydraulic fluid into and out of the strut, a double-wall annular tube was added outside the existing single-wall orifice support tube to form an annular passage from the new cylinder head, through the cylinder and orifice plate to the strut cavity. A line ran from the cylinder head, through a hand valve, to a quick-response servo-valve with position governed by an electronic controller. Inputs to the controller are signals from an upper-mass accelerometer; a linear potentiometer to measure instantaneous strut stroke; and a strut hydraulic pressure transducer. Other quantities needed by the controller are airplane mass and sink rate at touchdown. The function of the hand valve was to convert the system to the passive mode for comparison testing with the active mode.

This modified landing gear was installed in a specially-designed fixture on the front of a test carriage at the Langley Landing Loads Track (now called Aircraft Landing Dynamics Facility) as shown in Figure 14. The fixture basically consisted of a pitching beam supported in a vertical drop frame, the pitching beam being weighted and balanced to simulate the correct loading for the single main gear. Nose gear, wing lift, and elevator force simulators were incorporated in the drop frame as shown in Figure 14. A hydraulic power unit was installed to assure an adequate supply of high pressure hydraulic fluid. No attempt was made to optimize the hydraulic system. The combination of drop frame and carriage permitted simulation of a broad range of operational parameters, from 0 to 41 m/s (135 ft/s or 80 knots) forward speed and up to 1.8 m/s (6 ft/s) sink rate at touchdown. Following landing impact, the remainder of the test runway was used to study runout and taxi behavior over a rough surface, a smooth surface, and specially-installed step bumps.

A sample of test results is shown in Figure 15 for two test runs at 41 m/s (135 ft/s or 80 knots) forward speed, and a sink rate at touchdown of 1.7 m/s (5.5 ft/s). The actively controlled gear results are shown in solid lines, and the passive gear results are shown in dashed lines. Load reductions of 11% at impact and 36% during rebound were measured. These results were substantially less than predicted analytically or observed during vertical drop tests at zero forward speed. Differences are believed to be due to strut binding or stick-slip action ("stiction") caused by spin-up drag loads. Large reductions of load were observed in the rollout phase, and this feature could have an important influence on fatigue life. These load reductions are achieved at the expense of strut stroke. In some cases active strokes were as much as 250% greater than passive strokes. Measured active strokes, however, never exceeded 85% of available stroke.

The next stage of active landing gear research is planned to be a flight test on an F-106 aircraft. Plans are to outfit the aircraft with active controlled gear on both the main gears and the nose gear, and perform flight and taxi tests at Wallops Flight Test Station, Virginia. Currently, design of the control system and hydraulic system is in progress, and basic landing gear hardware has been acquired for this work.

V. Aircraft Landing Dynamics Facility

The Aircraft Landing Dynamics Facility (ALDF)[6], formerly called the Landing Loads Track, is capable of testing full-scale aircraft landing gear systems under closely controlled conditions on various runway-type surfaces. The facility originally became operational in 1956, and a three-year project to update and enhance its capabilities was completed in 1985. Testing at this facility has advantages over flight testing because of safety, economy, parameter control, and versatility. Essentially any landing gear can be accommodated in the test carriage including those exhibiting new concepts.

The facility is pictured in Figure 16. It consists of a concrete track test surface with a water-jet propulsion system on one end (the near end in Fig. 16) and a cable arrestment system on the other end (the far end in Fig. 16). Steel rails are on either side of the concrete track, and a truss-structure carriage which carries the test article is propelled down the track. The carriage has a truck on each of four corners with steel wheels which run on the rails. The original maximum speed capability was 204 km/hr (127 miles/hr or 110 knots) and the original track length was 670 m (2,200 ft). The purpose of the update project was to double the maximum speed capability to 407 km/hr (253 miles/hr or 220 knots) and extend the length of the track to 853 m (2,800 ft). A new carriage was designed and constructed to accomodate larger test articles and withstand higher acceleration loads. Finally, it was required to design-in the flexibility of using the old test carriage in addition to the new carriage. This requirement would allow test preparations on one carriage to be underway while testing is in progress using the other carriage. A brief review is presented here covering propulsion system, carriage, arrestment system, and proposed research.

Propulsion System

The propulsion system is pictured in Figure 17. It consists of an "L"-shaped vessel containing water pressurized by air. The high-pressure air is stored in three steel bottles and fed into the L-vessel through the goose neck pipe shown in Figure 17. The L-vessel contains 98.4 m^3 (26,000 gal) of water. On the end of the L-vessel away from the goose neck pipe is a high speed shutter valve which controls the water jet. When the shutter valve is opened the nozzle forms a water jet 0.46 m (18 in.) in diameter. The valve is operated with a hydraulic actuator. It can be opened in 0.4 s, held open for a prescribed dwell time, and then closed in 0.3 s. The dwell time can range from 0 s to 0.9 s, and the air pressure in the storage bottles can be adjusted to produce a variety of testing speeds. At the maximum air pressure of 21.7 MPa (3150 psi) the water jet produces a thrust of approximately 8.9 MN (2.0 Mlbf) on the carriage. The carriage mass is 49,000 kg (108,000 lbm), and the water jet thrust develops a peak acceleration of 20 G. The carriage accelerates from zero velocity to 407 km/hr (253 miles/hr or 220 knots) in 120 m (400 ft) and 2 s.

Carriage

A photograph of the new carriage is shown in Figure 18. It is a truss structure constructed of tubular steel members and contains a central open

bay 12 m (40 ft) long and 6 m (20 ft) wide in which a variety of test articles can be mounted. On the aft end of the carriage is mounted a turning bucket 3 m (10 ft) high and 1 m (3 ft) wide. The bucket captures the water jet from the L-vessel and turns it through an angle of 170 degrees. The momentum exchange involved in this process supplies the thrust which accelerates the carriage. On the forward end of the carriage is a nose block that intercepts five arresting cables stretched across the track at the arrestment end. In the central bay of the carriage is a drop frame on which test articles are mounted. The drop frame rides on four vertical rails, and two hydraulic lift cylinders lower or raise the test article and apply vertical loads as required by the test program.

Arrestment System

A sketch of the arrestment system is shown in Figure 19. Concrete foundations located on either side of the track support five arresting devices each. An arresting device consists of a tub of water containing rotor and stator vanes. The rotor is attached to a rotating shaft which protrudes through the top of the tub, and a spool is attached to each rotating shaft. Nylon tapes 20 cm (8 in.) wide and 1 cm (3/8 in.) thick are wound onto each spool. The tapes, in turn, are attached to five cables which cross the track and pick up the nose block on the carriage. As the carriage pulls tape from the spools, the rotor vanes churn the water in the tubs. This churning action converts carriage kinetic energy into heat, which is absorbed into a water reservoir. The arrestment system is designed to stop the carriage in 150 m (500 ft) even if only three of the five sets of cables and devices are operating.

Research Program

The updated ALDF became operational in August 1985. The first research program involves measuring Shuttle Orbiter main and nose gear tire spin-up wear and cornering force characteristics at high speeds. Future research will include developing data on frictional characteristics of radial and H-type aircraft tires for comparison with conventional bias ply tires. This radial and H-type tire program is a joint effort among NASA, Federal Aviation Administration (FAA), U.S. Air Force, Society of Automotive Engineers, and the U.S. tire industry. A third program is a joint NASA-FAA runway surface traction program to study effects of different runway surface texture and grooving patterns on stopping and steering characteristics of aircraft tires. With its upgraded capability, the ALDF is equipped to conduct research on present and future landing gear systems under realistic operational conditions. These three programs plus additional planned work are expected to provide a full research agenda for the next five years.

VI. Concluding Remarks

Recent research is reviewed on three topics: cornering forces generated by aircraft tires on a tilted or cambered, free-swiveling nose gear; spray ingestion from aircraft nose gear; and actively controlled landing gear. Cornering forces on tilted nose gear were measured on a research test frame, a fighter aircraft, and the Space Shuttle Orbiter. These data are significant in simulating or predicting aircraft ground operations. Measurements were made of spray patterns emanating from a nose wheel operating on a flooded runway. Limited understanding of the characteristics of the spray behavior was developed for general aviation aircraft. Actively controlled landing gear technology has advanced to the point where a flight test is planned. This technology appears to offer benefits in operations over damaged and repaired runways, reduced fatigue damage, and improved ride qualities for large, flexible aircraft. Finally, a description of a unique updated aircraft landing dynamics research facility recently placed into operation at Langley Research Center is presented.

References

1. Stubbs, Sandy M.: Landing Characteristics of a Dynamic Model of the HL-10 Manned Lifting Entry Vehicle. NASA TN D-3570, 1966.

2. Daugherty, Robert H.: A Study of the Cornering Forces Generated by Aircraft Tires on a Tilted, Free-Swiveling Nose Gear. NASA TP 2481, October 1985.

3. Stubbs, Sandy M. and Tanner, John A.: Technique for Measuring Side Forces on a Banked Aircraft With a Free-Swiveling Nose Gear. NASA TM 87719, 1986.

4. McGehee, John R. and Carden, Huey D.: A Mathematical Model of an Active Control Landing Gear for Load Control During Impact and Roll-Out. NASA TN D-8080, 1976.

5. McGehee, John R. and Dreher, Robert C.: Experimental Investigation of Active Loads Control for Aircraft Landing Gear. NASA TP 2042, 1982.

6. Davis, Pamela A.; Stubbs, Sandy M.; and Tanner, John A.: Aircraft Landing Dynamics Facility, A Unique Facility with New Capabilities. SAE Technical Paper 851938. Presented at Society of Automotive Engineers Aerospace Technology Conference and Exposition, Long Beach, California, October 14-17, 1985.

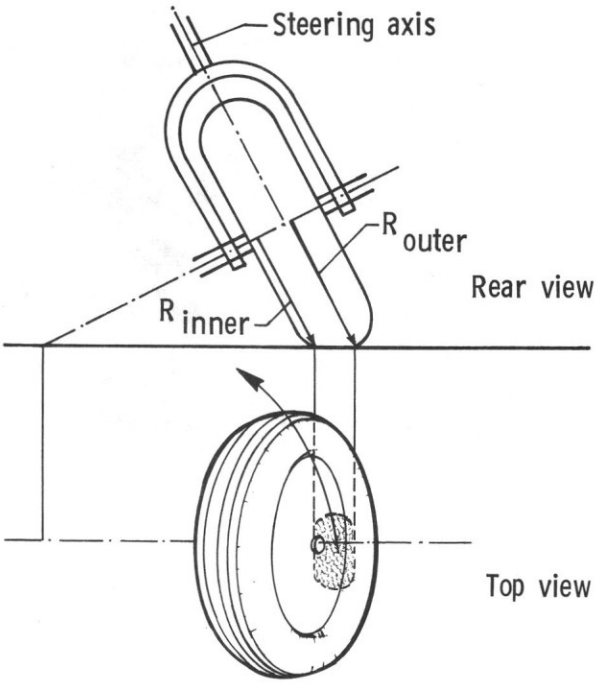

Figure 1. Tilt Steering Phenomenon

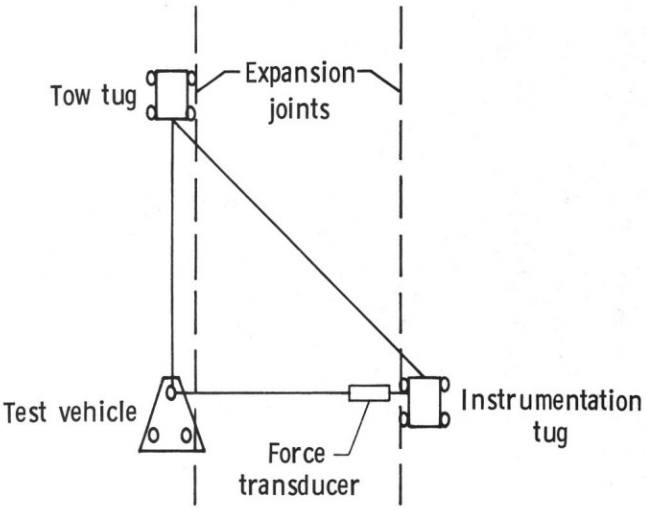

Figure 3. Schematic of Tow Test Setup for Tilt Steering Research

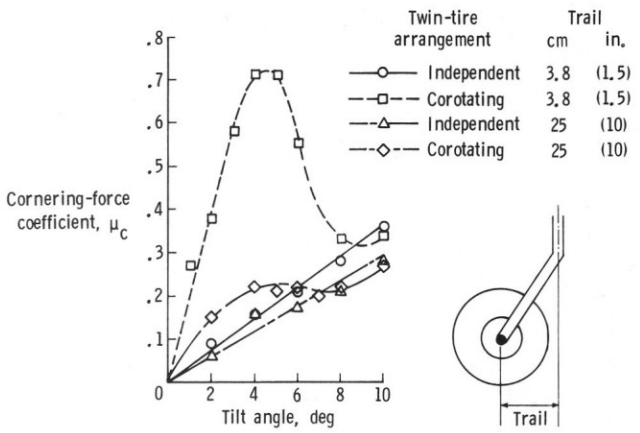

Figure 4. Cornering-Force Coefficient as a Function of Tilt Angle for Various Twin-Tire and Trail Arrangements

Figure 2. Airboat Test Frame for Tilt Steering Research

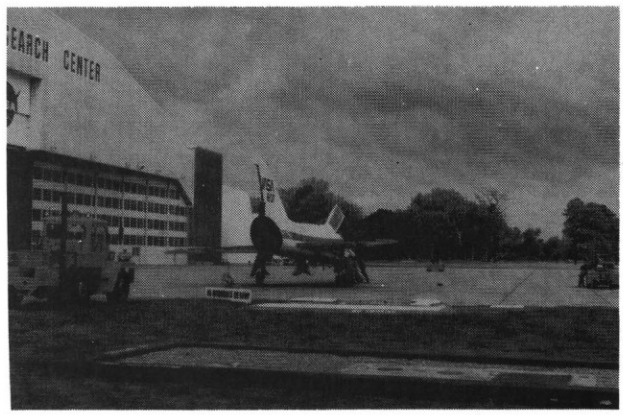

Figure 5. F-106 Tow Test Setup for Tilt Steering Research

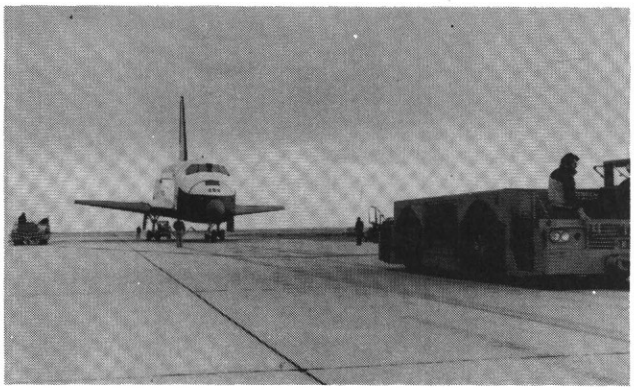

Figure 6. Space Shuttle Orbiter Tow Test Setup for Tilt Steering Research

Figure 8. Turbine-powered Aircraft Experiences Nose Wheel Water Spray

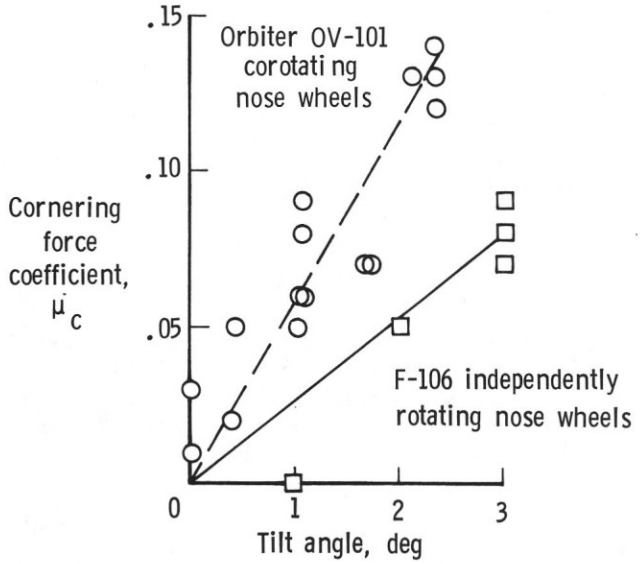

Figure 7. Cornering-Force Coefficient as a Function of Tilt Angle for F-106 and Shuttle Orbiter

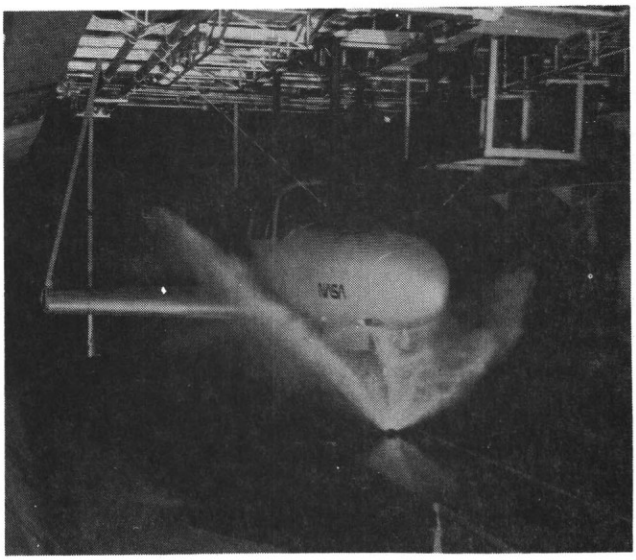

Figure 9. Nose Wheel Spray Testing in Towing Tank

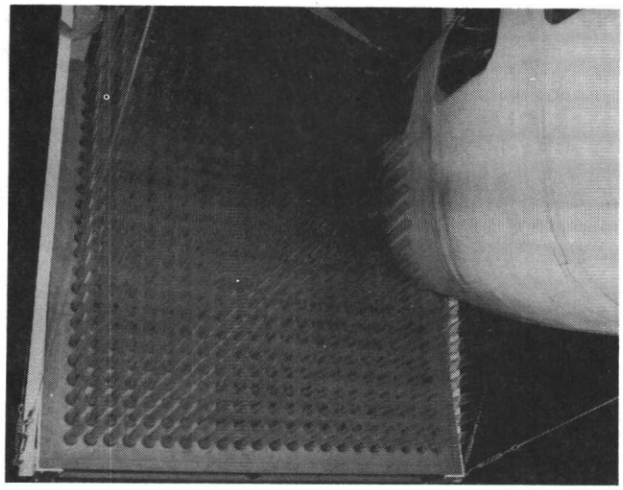

Figure 10. Water Collection Apparatus for Spray Ingestion Testing

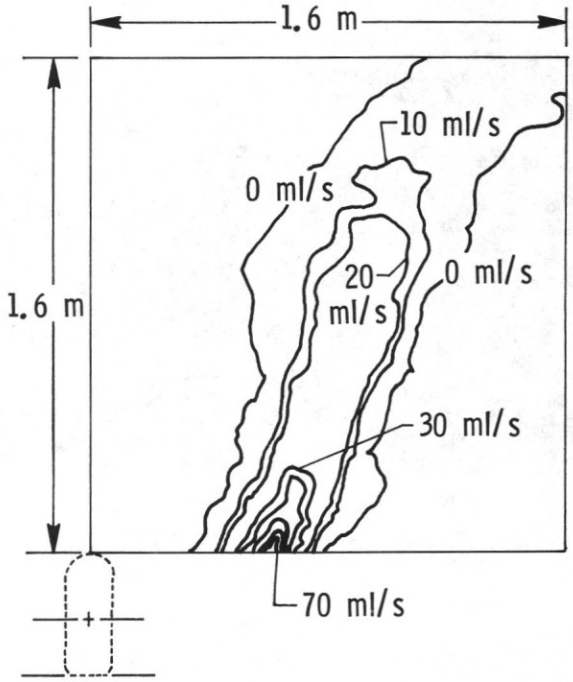

Figure 12. Contour Map of Flow Rate Measurements for Nose Wheel Spray

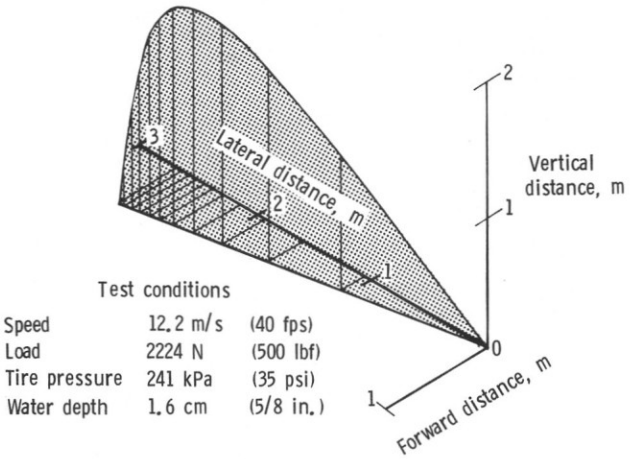

Figure 11. Typical Estimated Spray Droplet Trajectory

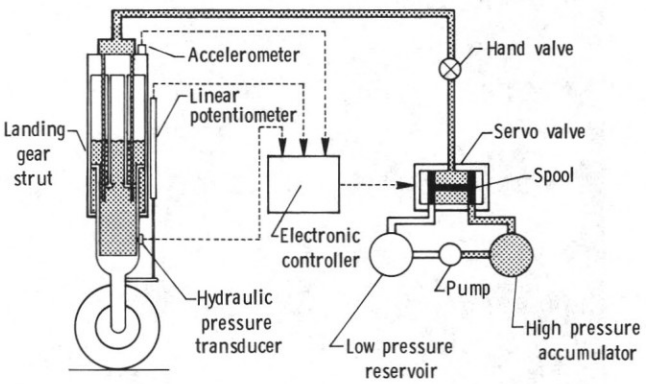

Figure 13. Schematic of Active Controlled Landing Gear Experimental Setup

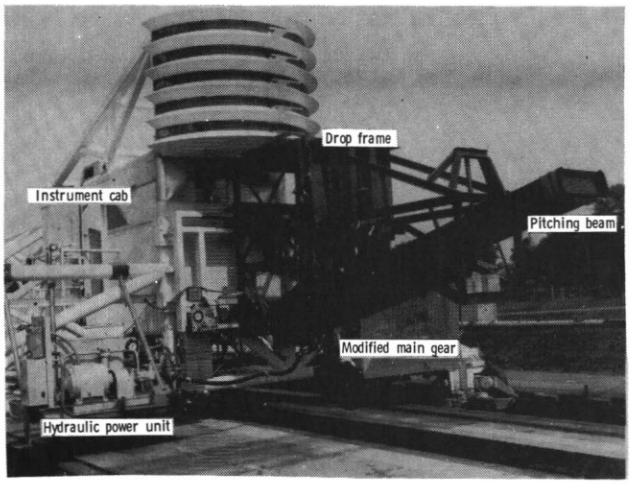

Figure 14. Test Fixture Mounted on Landing Loads Track Carriage for Active Controlled Landing Gear Research

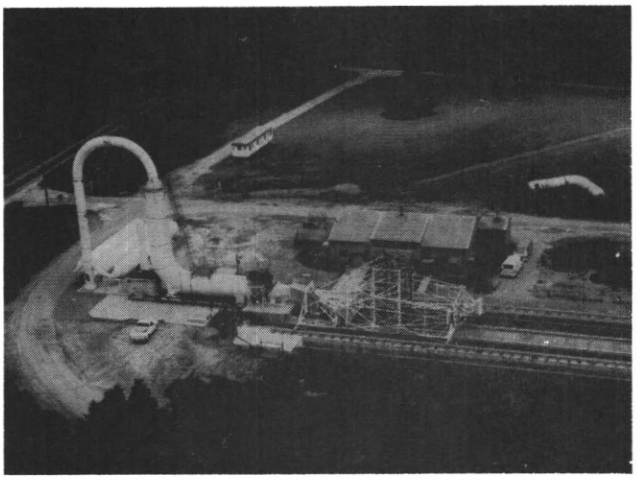

Figure 17. Aircraft Landing Dynamics Facility Propulsion System

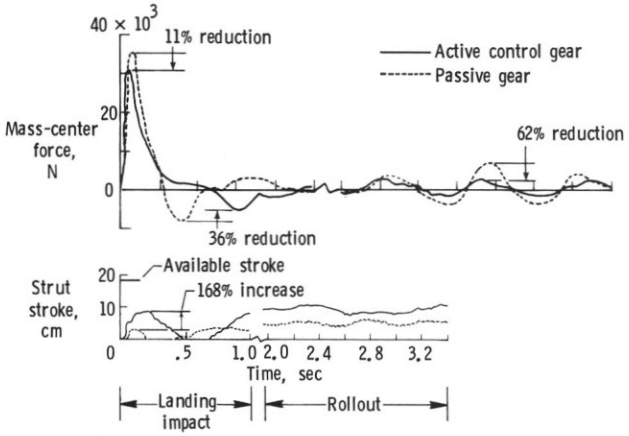

Figure 15. Results From Active Controlled Landing Gear Tests on Landing Loads Track

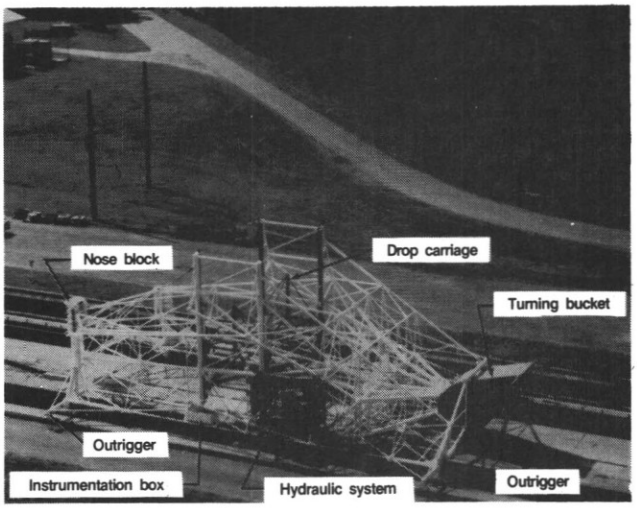

Figure 18. Aircraft Landing Dynamics Facility Carriage

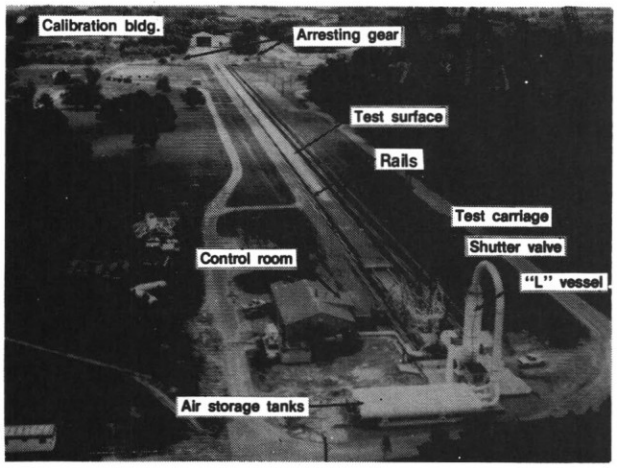

Figure 16. Aircraft Landing Dynamics Facility

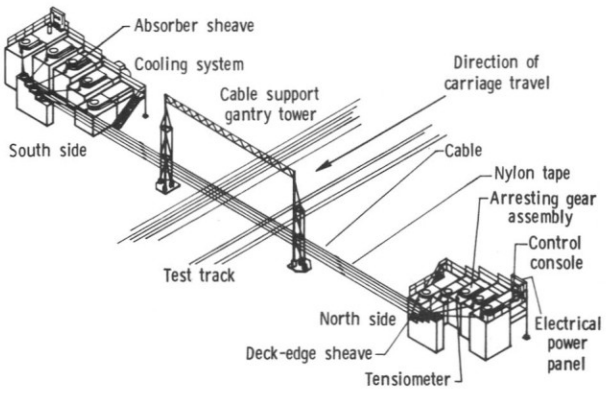

Figure 19. Aircraft Landing Dynamics Facility Arrestment System